Electronic supplementary information (ESI)

Synthesis, Crystal Structure and Investigation of Ion-Exchange Possibility for Sodium Tellurate $NaTeO_3(OH)$

Tsubasa Ishii,[a] Yue Jin Shan,[a,*] Kotaro Fujii,[b] Tetsuhiro Katsumata,[c] Hideo Imoto,[a] Ariunaa Baterdene,[d] Keitaro Tezuka [a] and Masatomo Yashima [b]

a. Division of Engineering and Agriculture, Graduate School of Regional Development and Creativity, Utsunomiya University, Tochigi 321-8585, Japan
b. Department of Chemistry, School of Science, Tokyo Institute of Technology, Tokyo 152-8551, Japan
c. Department of Chemistry, School of Science, Tokai University, Kanagawa 259-1292, Japan
d. Graduate School of Science and Technology, Gunma University, Gunma 376-8515, Japan

*Corresponding author: shan@cc.utsunomya-u.ac.jp

Supporting text

Text S1

The generalized gradient approximation (GGA) electronic calculation was carried out with Quantum ESPRESSO. The optimized structure of $NaTeO_3(OH)$ was studied through an electronic calculation using the projector augmented wave (PAW) potentials for Na, Te, O and H atoms. A plane-wave basis set with a cutoff of 47 Ry was used. The Perdew-Burke-Ernzerhof (PBE) GGA was employed for the exchange and correlation functionals. Sums over occupied electronic states were performed using the Monkhorst-Pack scheme on a 6 × 3 × 6 set of a k-point mesh. Unit-cell parameters and atomic coordinates were optimized with the convergence condition of 10^{-6} Ry. The positions of all atoms were relaxed in the space group $P2_1/a$.

Text S2

Several analytical experiments were performed to analyze the composition of the synthesized sodium tellurate. First, atomic absorption spectroscopy was used to determine the ratio of Na to Te cations in the sample. The analysis results indicate that there is a 1:1 ratio between the Na and Te cations. Next, the IR spectrum of the sample was measured and characteristic peaks were observed. These peaks were caused by stretching vibration (3000 cm^{-1}) and bending vibration (1200 cm^{-1}) of OH groups. The presence of OH groups in the sodium tellurate was confirmed. Thermogravimetric-differential thermal analysis (TG-DTA) was performed for further investigation. Before the experiment, the samples were dried at 120°C for over 48 hours to evaporate adsorbed water on the surface and between layers. The study was carried out by heating 50.05 mg of the sample in dry air at a rate of 5°C/min from room temperature to 600°C in a platinum container. As shown in Fig. S2, the sample experienced thermal decomposition at approximately 500°C, resulting in a weight change of -2.12 mg (weight loss: 4.24 wt%). Consequently, the final weight of the sample was 47.93 mg. The XRD pattern of the product after heating matched that of $Na_2Te_2O_7$ (ICSD: 391382[43]) as shown in Fig. S3. Since there was no change in the oxidation state of the cations before and after heating, it can be inferred that the oxygen content of the sample did not increase or decrease during the heating process, only the water (or OH group) was removed. Thus, the amount of water removed is estimated to be 0.1177 mmol. This is nearly the same amount as the $Na_2Te_2O_7$ formed after heating, which was calculated to be 0.1160 mmol based on the weight of the final sample. The analysis indicates that the sodium tellurate comprises $Na_2Te_2O_7$ and H_2O in equal proportions, with a ratio of 1 : 1 as expressed by the following equation:

$$Na_2Te_2O_7 + H_2O \rightarrow 2NaTeO_3(OH)$$

The obtained sodium tellurate was found to have a chemical formula of $NaTeO_3(OH)$.

Text S3

The density of the synthesized sodium tellurate $NaTeO_3(OH)$ was measured using a 5 mL Gay-Lussac pycnometer. The density data for the samples, measured at a water temperature of 19 °C, is presented in Table S3. The number (Z) of $NaTeO_3(OH)$ units in the unit cell was calculated using the lattice constant and density values of the $NaTeO_3(OH)$ sample according to the following equation:

$$Z = \frac{unit\ cell\ volume(cm^3) \times density(g/cm^3)}{formula\ weight(g/mol) \times Avogadro\ constant(mol^{-1})}$$

Since the estimated Z is 4.10, the Z of the novel sodium tellurate is determined to be 4.

Table S1 Experimental results of density measurement

	calculation process	1st	2nd	3rd
pycnometer (g)	A	10.95750	10.95811	10.95814
pycnometer filled with water_1 (g)	B	17.21712	17.20890	17.20874
pycnometer containing sample (g)	C	11.83054	11.87690	11.81265
pycnometer filled with sample and water_2 (g)	D	17.88857	17.91556	17.86680
mass of sample (g)	C-A	0.87304	0.91879	0.85451
mass of water_1 (g)	B-A	6.25962	6.25079	6.25060
mass of water_2 (g)	D-C	6.05803	6.03866	6.05415
volume of sample (cm^3)	[(B-A)-(D-C)]/0.9984#	0.20191	0.21247	0.19676
measured density (g/cm^3)	C-A/[(B-A)-(D-C)]/0.9984	4.3238	4.3243	4.3428
average measured density ± standard deviation		4.33 ± 0.01		

#: the density of water at 19°C [52]

Text S4

The space groups $P2_1/c$ and $P2_1/a$ for $NaTeO_3(OH)$ were estimated using the analysis software EXPO2014 and synchrotron XRD data. The lattice constants of the two estimated space groups are identical, with a value of the a = 5.66354 Å, b = 11.96795 Å, c = 5.02543 Å and β = 95.4336°. The atomic coordinates for each are displayed in Table S2. Fig. S10 demonstrates that in both space groups, the one-dimensional chains of TeO_6 octahedra extend along the c-axis and originate from different points. Black and red lines indicate the unit cells of the space groups $P2_1/c$ and $P2_1/a$, respectively. There is no difference in the arrangement of atoms in either space group when viewed from the b-axis. However, there are two types of one-dimensional chains (Queue 1 and 2) with different y-coordinates. The central position of Queue 1 in $P2_1/c$ is approximately at y = 3/4, while the central position of Queue 2 is approximately at y = 1/4. In contrast, the central position of Queue 1 in $P2_1/a$ is nearly at y = 1/2, and the central position of Queue 2 is nearly at y = 0. The origin cannot be shifted by (1/4, 1/4, 1/4) to align the unit cells of two different space groups. In other words, the crystal structures of $P2_1/c$ and $P2_1/a$ have different unit cells. The glide planes perpendicular to the b-axis of $P2_1/c$ and $P2_1/a$ have different directions, which are believed to cause slight variations in the coordinates of each atom. These variations result in differences in the diffraction patterns. Finally, the simulated patterns for each space group were compared with the actual measured pattern, and the space group $P2_1/a$ was identified that had the simulation pattern closest to the actual measurement pattern.

Table S2 Estimated structural parameters of $NaTeO_3(OH)$.

a = 5.66354 Å, b = 11.96795 Å, c = 5.02543 Å, β = 95.4336°						
	$P2_1/c$			$P2_1/a$		
	x	y	z	x	y	z
Te	0.7479	0.16418	0.01814	0.0084	0.42727	0.2514
Na	0.21543	0.0907	0.47671	0.472	0.65301	0.219
O1	-0.07055	0.0623	0.17321	-0.2005	0.53988	0.046
O2	0.51591	0.08357	0.82909	0.1698	0.55319	0.4563
O3	0.94217	0.20047	0.7153	0.2404	0.33284	0.4204
O4	0.56791	0.2086	0.31533	-0.16879	0.3118	0.0881

Table S3 Optimized structural parameters of $NaTeO_3(OH)$ by DFT calculation and the migration distance of each atom before and after the calculation.

			DFT Calculation $P2_1/a$ (No.14) a = 5.66813 Å, b = 12.02570 Å c = 5.08224 Å, β = 95.2815°			Neutron Refinement $P2_1/a$ (No.14) a = 5.66164 Å, b = 11.97263 Å c = 5.02554 Å, β = 95.3948°			The difference of DFT calculation and Neutron Refinement			
atom	site	g	x	y	z	x	y	z	$a\,\Delta x$/Å*	$b\,\Delta y$/Å*	$c\,\Delta z$/Å*	distance/Å**
Na(1+)	4*e*	1	0.48074	0.65122	0.20806	0.4876	0.6568	0.2145	-0.0388	-0.0668	-0.0324	0.082
Te(6+)	4*e*	1	0.01012	0.42687	0.25093	0.0113	0.42726	0.2507	-0.0067	-0.0047	0.0012	0.008
O1(2-)	4*e*	1	0.79599	0.53929	0.04482	0.80121	0.54151	0.04839	-0.0296	-0.0266	-0.0179	0.042
O2(2-)	4*e*	1	0.18055	0.55569	0.44500	0.17129	0.55191	0.44557	0.0524	0.0453	-0.0029	0.070
O3(2-)	4*e*	1	0.24332	0.32880	0.42634	0.23401	0.33529	0.42344	0.0527	-0.0777	0.0146	0.094
O4(2-)	4*e*	1	0.33230	0.19103	0.08996	0.33416	0.19111	0.09122	-0.0105	-0.0010	-0.0063	0.012
H(1+)	4*e*	1	0.28171	0.26636	0.71860	0.2636	0.2769	0.2698	0.1025	-0.1262	0.1035	0.188

*The cell parameters of neutron rietveld analysis are used.

** These values were calculated using the formula: $distance^2 = (a\,\Delta x)^2 + (b\,\Delta y)^2 + (c\,\Delta z)^2 + 2(a\,\Delta x)(c\,\Delta z)\cos\beta$

Table S4 Refined structural parameters of $KTeO_3(OH)$ and the BVS results for each ion.

Chemical formula	$KTeO_3(OH)$
Crystal system	Monoclinic
Space group	$P2_1/a$, No.14, Z = 4
Lattice parameters (Å)	a = 6.500670(12)
	b = 11.700423(16)
	c = 5.123357(6)
	β = 93.85754(11)
Volume (Å^3)	388.8026(6)
Calculated density (g/ cm^3)	3.96
R_{wp}	1.52%
R_B	3.51%
R_F	2.21%
S	1.88

atom	site	g	x	y	z	B (Å^2)	BVS*
K(1+)	4*e*	1	0.4812(2)	0.65724(6)	0.2392(3)	0.970(16)	1.05
Te(6+)	4*e*	1	0.00563(16)	0.42712(4)	0.2502(2)	0.425(8)	5.81
O1(2-)	4*e*	1	0.83859(12)	0.54541(6)	0.05092(16)	0.440(4)	1.99
O2(2-)	4*e*	1	0.15609(11)	0.55367(7)	0.44163(16)	0.440(4)	1.95
O3(2-)	4*e*	1	0.20452(10)	0.32502(6)	0.40569(13)	0.440(4)	2.14
O4(2-)	4*e*	1	0.34187(10)	0.18627(6)	0.09876(13)	0.440(4)	1.86
H(1+)	4*e*	1	0.25218(18)	0.27234(8)	0.2675(2)	0.573(16)	1.07

*: The BVS values were calculated by softBV.

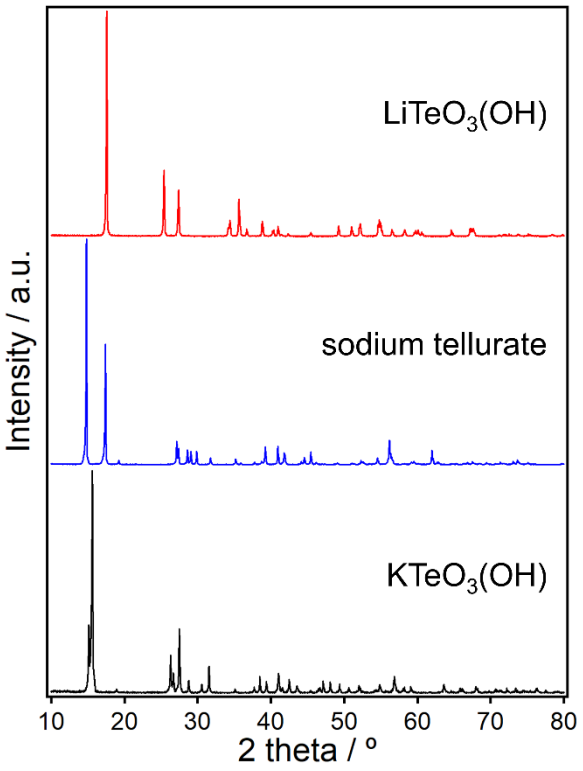

Fig. S1 XRD patterns of lithium tellurate $LiTeO_3(OH)$, sodium tellurate and potassium tellurate $KTeO_3(OH)$.

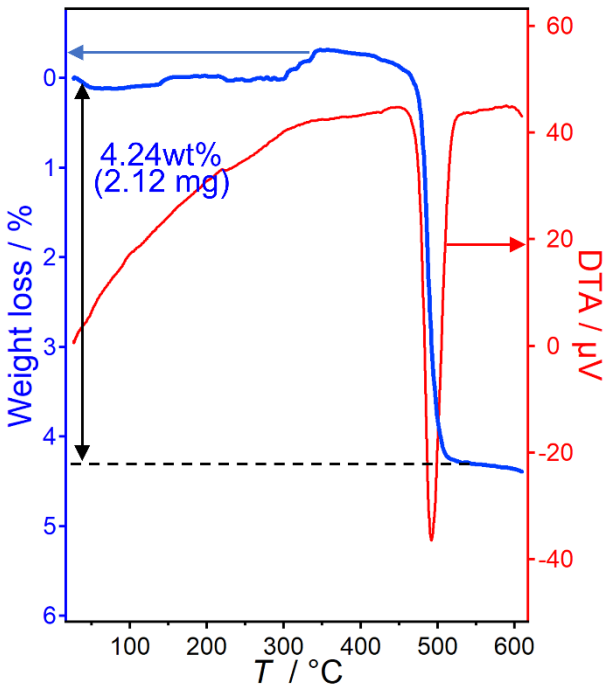

Fig. S2 TG-DTA curve for the synthesized sodium tellurate. TG-DTA measurement was performed using a platinum vessel. The sample was heating in air from room temperature to 600°C at a heating rate of 5°C/min.

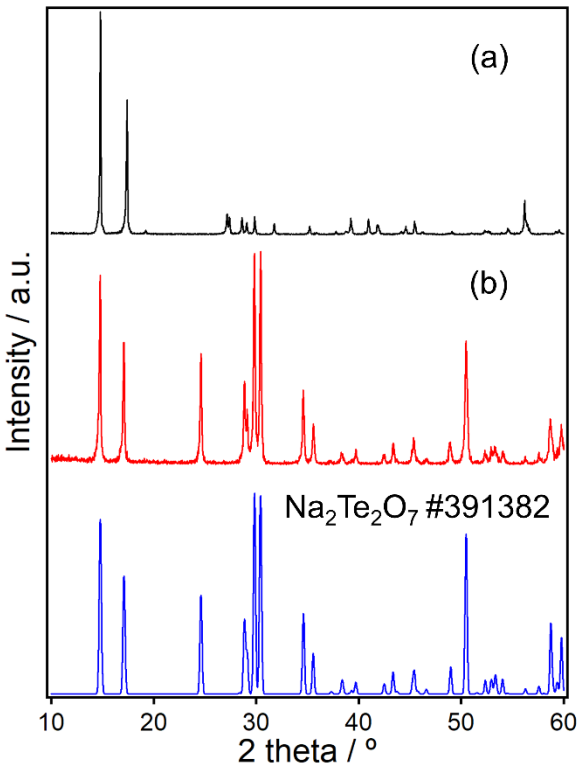

Fig. S3 XRD patterns of a synthesized sodium tellurate before (a) and after (b) being heated to 500°C for 2 h. The ICSD pattern (ICSD: 391382 [43]) for $Na_2Te_2O_7$ is added for comparison.

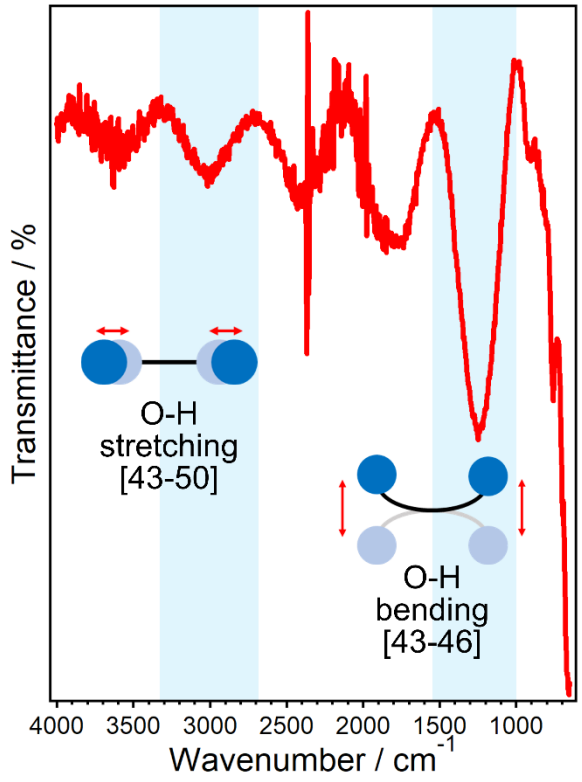

Fig. S4 ATR-FTIR spectrum of synthesized sodium tellurate.

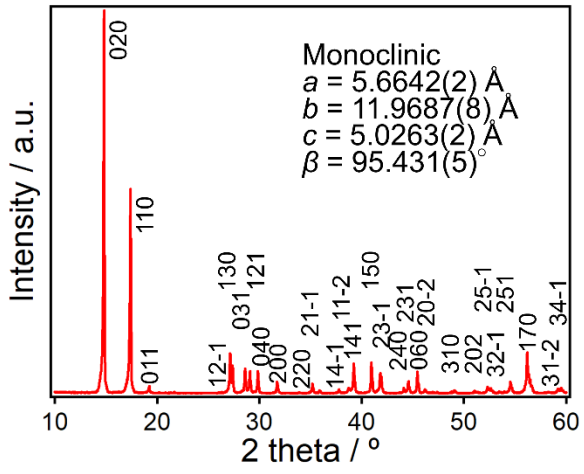

Fig. S5 Indexed XRD pattern of synthesized sodium tellurate.

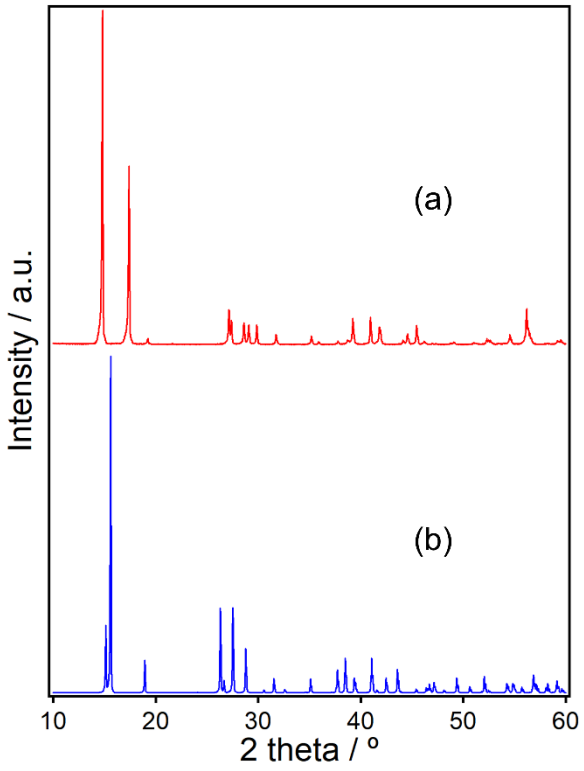

Fig. S6 Observed XRD pattern of $NaTeO_3(OH)$ (a) and simulation pattern (b) using the crystal structure of $KTeO_3(OH)$ as a model structure.

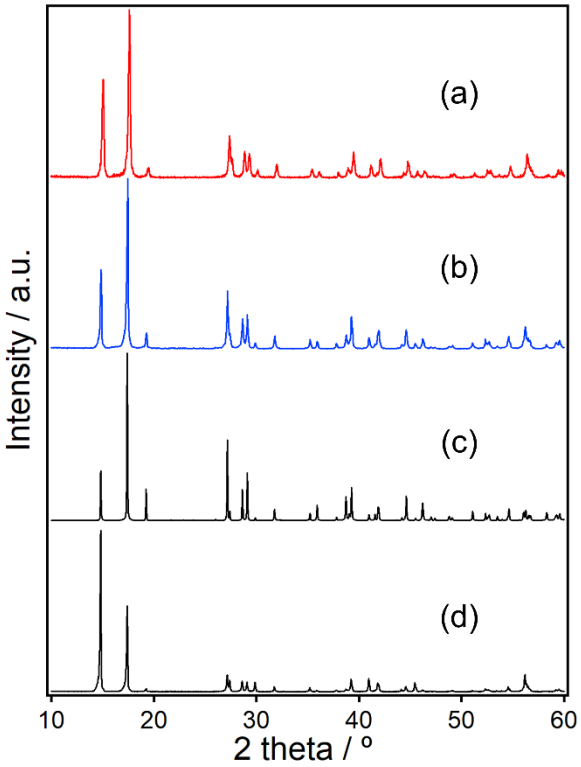

Fig. S7 XRD patterns of $NaTeO_3(OH)$ samples mixed with adhesive (Aron Alpha (Toagosei) (a), C (Cemedine) (b)). Synchrotron XRD pattern (c) and laboratory XRD pattern (d) of $NaTeO_3(OH)$ are added for comparison.

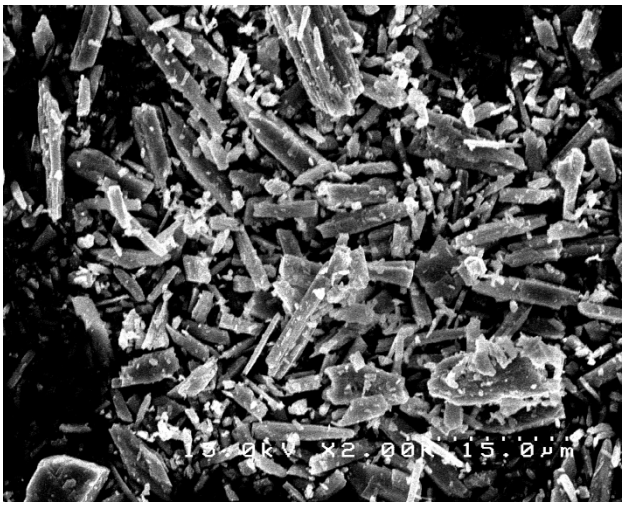

Fig. S8 FE-SEM image of the obtained $NaTeO_3(OH)$.

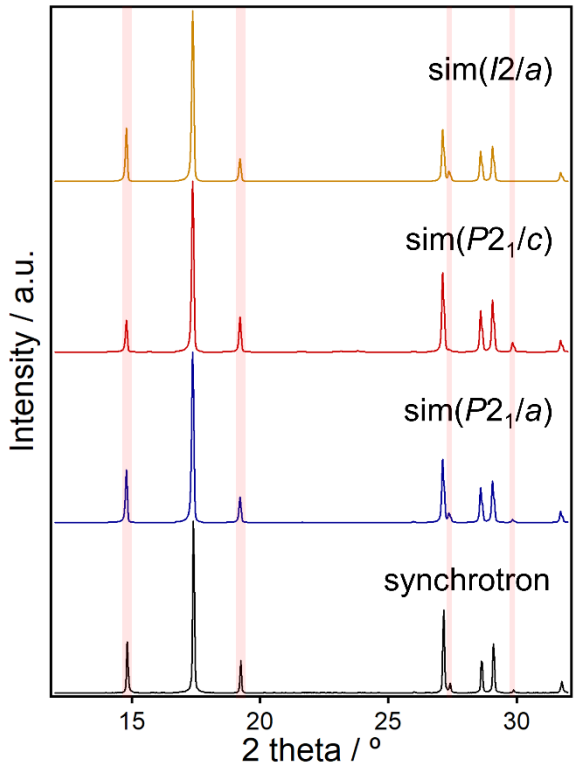

Fig. S9 Synchrotron XRD pattern of $NaTeO_3(OH)$ and simulated XRD patterns using three space groups.

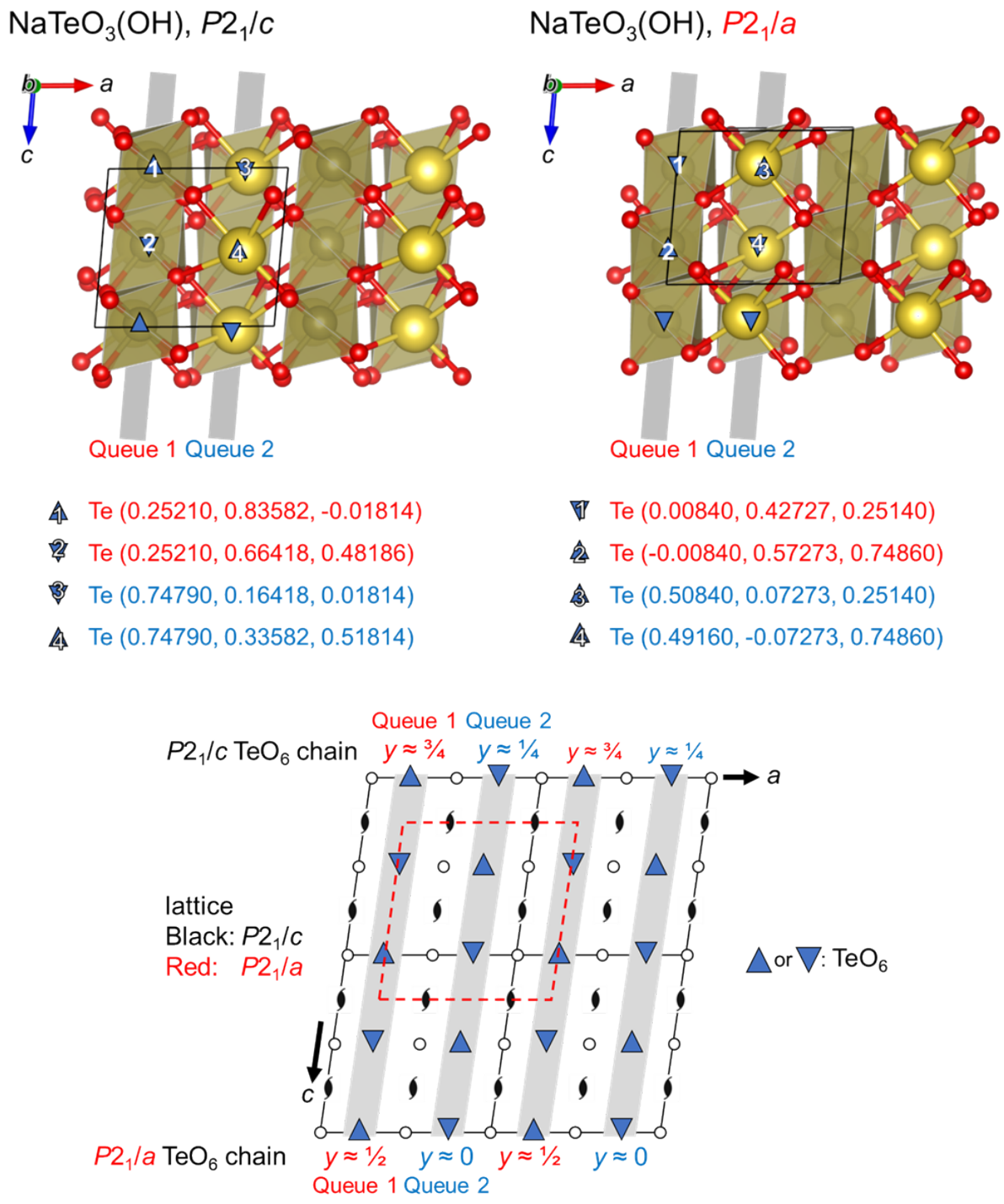

Fig. S10 Explanation of the differences between $P2_1/c$ and $P2_1/a$.

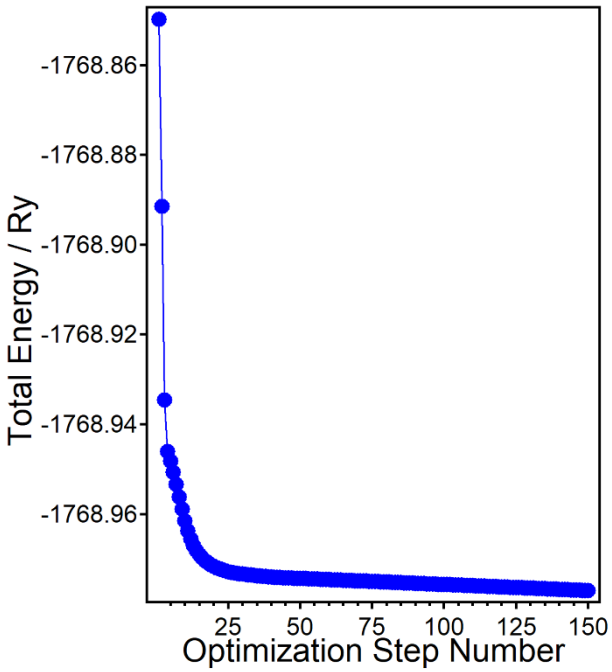

Fig. S11 Total energy change during optimization of $NaTeO_3(OH)$ at each step.

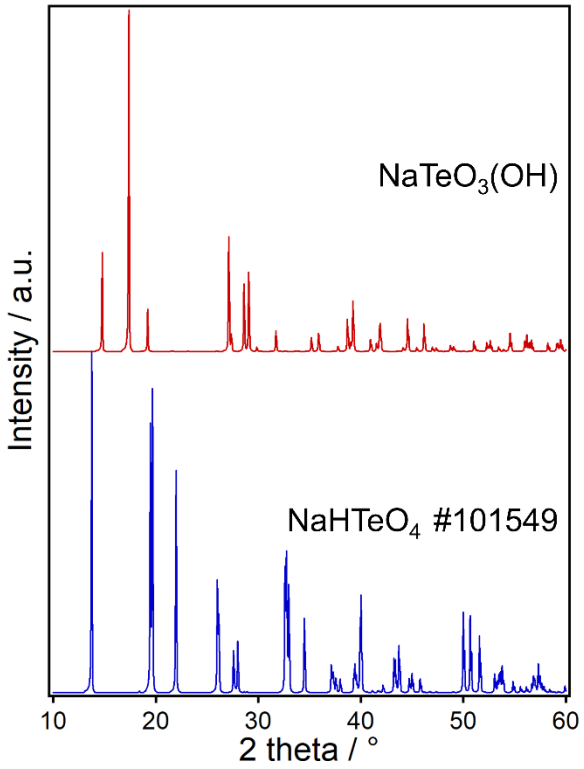

Fig. S12 Simulated patterns of $NaTeO_3(OH)$ (this study) and $NaHTeO_4$ (ICSD: 101549 [33]).

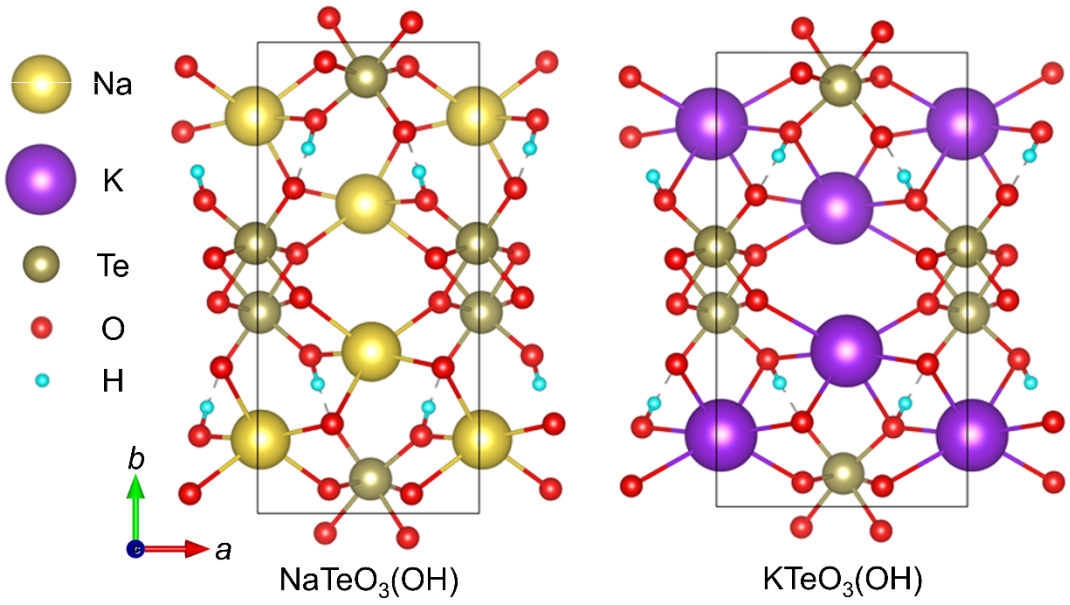

Fig. S13 Crystal structure of $NaTeO_3(OH)$ and $KTeO_3(OH)$.

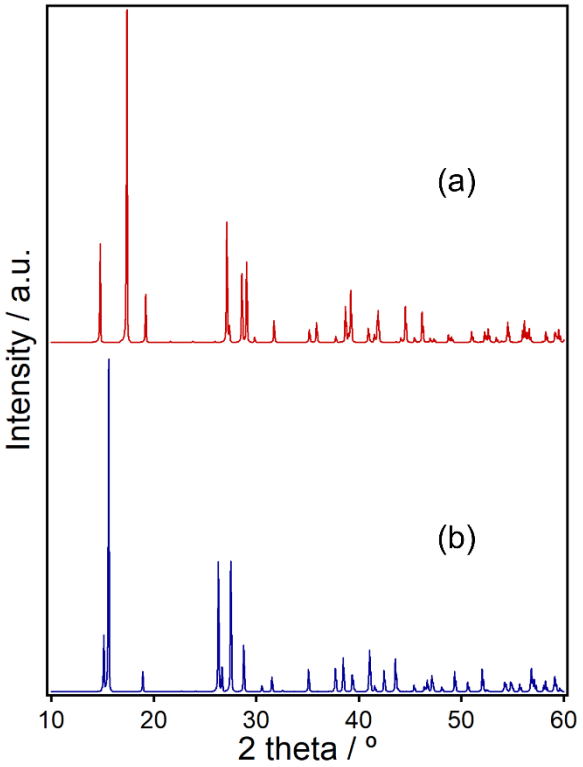

Fig. S14 XRD patterns of $NaTeO_3(OH)$ (a) and $KTeO_3(OH)$ (b).

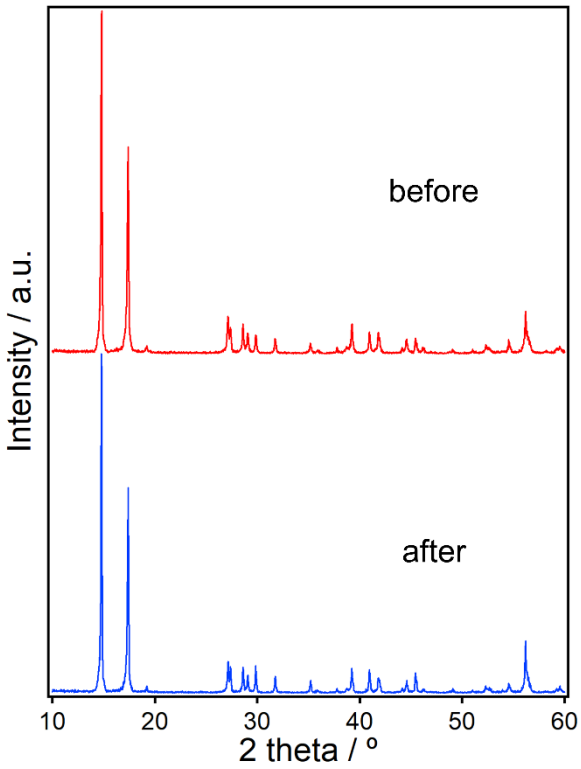

Fig. S15 XRD patterns of $NaTeO_3(OH)$ samples of before and after ion exchange experiments.

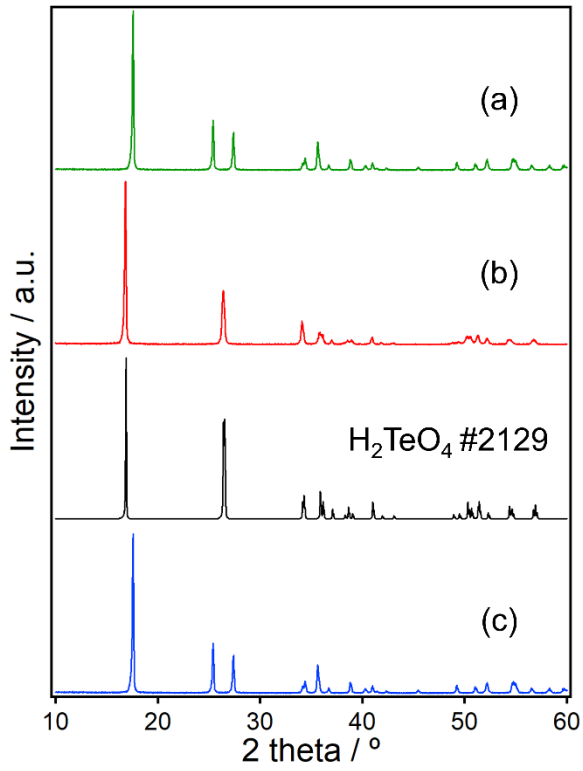

Fig. S16 XRD patterns of $LiTeO_3(OH)$ samples before(a) and after(b), as well as the reverse ion exchange(c). The ICSD pattern (ICSD: 2129 [61]) for H_2TeO_4 is added for comparison.

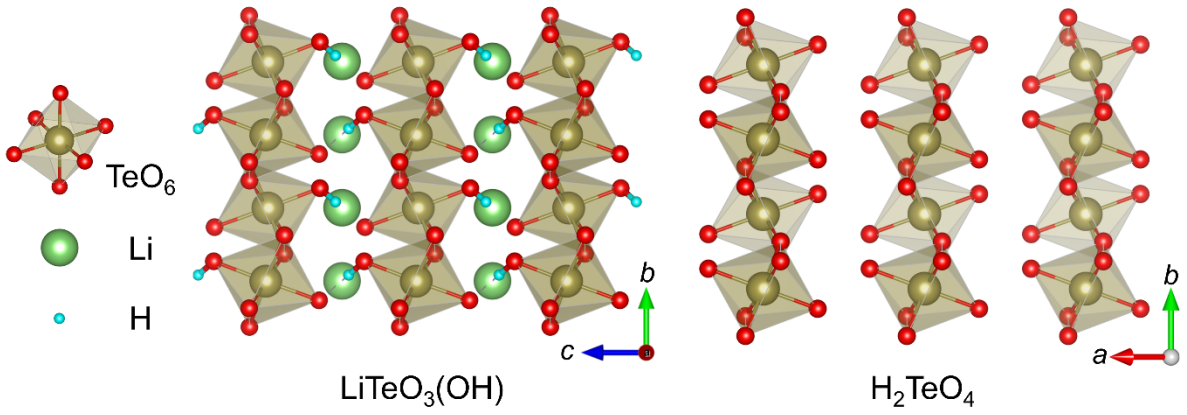

Fig. S17 Crystal structure of $LiTeO_3(OH)$ and H_2TeO_4.

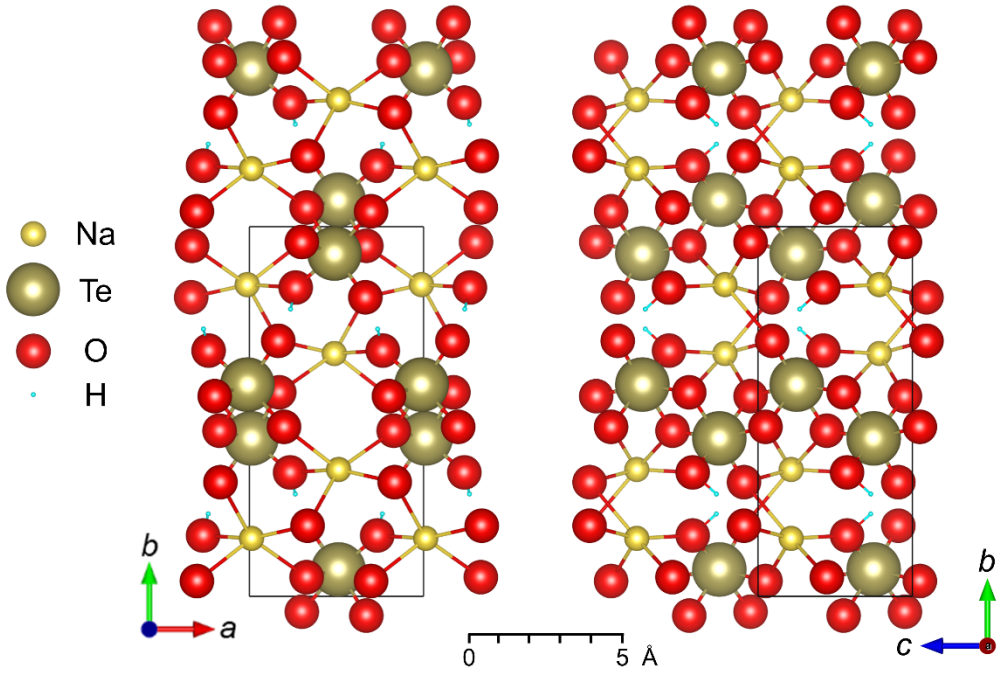

Fig. S18 Crystal structure of $NaTeO_3(OH)$ indicated by the ionic radius.